Insights into the influence of the Ag loading on Al2O3 in the H2-assisted C3H6-SCR of NOx

Tesnim Chaieb, Laurent Delannoy, Guylène Costentin, Catherine Louis, Sandra Casale, Ruth L. Chantry, Z.Y. Li, Cyril Thomas

Applied Catalysis B: Environmental 156–157 (2014) 192–201

Contents lists available at ScienceDirect

Applied Catalysis B: Environmental

journal homepage: www.elsevier.com/locate/apcatb

Insights into the influence of the Ag loading on Al_2O_3 in the H_2-assisted C_3H_6-SCR of NO_x

Tesnim Chaieb[a,b], Laurent Delannoy[a,b], Guylène Costentin[a,b], Catherine Louis[a,b], Sandra Casale[a,b], Ruth L. Chantry[c], Z.Y. Li[c], Cyril Thomas[a,b,*]

[a] Sorbonne Universités, UPMC Univ Paris 06, UMR 7197, Laboratoire de Réactivité de Surface, 4 Place Jussieu, F-75005 Paris, France
[b] CNRS, UMR 7197, Laboratoire de Réactivité de Surface, 4 Place Jussieu, F-75005 Paris, France
[c] Nanoscale Physics Research Laboratory, School of Physics and Astronomy, University of Birmingham, Edgbaston, Birmingham B15 2TT, United Kingdom

ARTICLE INFO

Article history:
Received 8 January 2014
Received in revised form 7 March 2014
Accepted 11 March 2014
Available online 20 March 2014

Keywords:
Ag/Al_2O_3
H_2 effect
Selective catalytic reduction
Kinetics
Compensation phenomenon

ABSTRACT

The addition of H_2 has been reported to promote drastically the selective catalytic reduction of NO_x by hydrocarbons (HC-SCR). Yet, the influence of the Ag loading on the H_2-promoted HC-SCR has been the subject of a very limited number of investigations. The H_2-HC-SCR earlier studies reported mostly on Ag/Al_2O_3 samples containing about 2 wt% Ag, since this particular loading has been shown to provide optimum catalytic performances in the HC-SCR reaction in the absence of H_2. The present study highlights for the first time that the H_2-C_3H_6-SCR catalytic performances of Ag/Al_2O_3 samples improved in the 150–550 °C temperature domain as the Ag loading (Ag surface density: x ($Ag/nm^2_{Al_2O_3}$)) decreased well below 2 wt%. A detailed kinetic study of H_2-C_3H_6-SCR was performed in which the reaction orders in NO, C_3H_6 and H_2, and the apparent activation energies were determined for the reduction of NO_x to N_2 on a $Ag(x)/Al_2O_3$ catalysts series, for which Ag was found to be in a highly dispersed state by TEM and HAADF-STEM. Remarkably, changes in these kinetic parameters were found to occur at an Ag surface density close to 0.7 $Ag/nm^2_{Al_2O_3}$ (Ag loading of 2.2 wt%) coinciding with the changes observed earlier in the NO_x uptakes of the Al_2O_3 supporting oxide [18]. Interpretation of the activity and kinetic data led us to conclude that the H_2-C_3H_6-SCR reaction proceeds via the activation of H_2 and C_3H_6 on Ag species and their further reaction with NO_x adspecies activated on the Al_2O_3 support. The unexpected higher catalytic performances of the Ag samples with the lower Ag surface densities was attributed to the higher concentration of active sites on the Al_2O_3 supporting oxide able to chemisorb NO_x species, in agreement with the NO_x uptake data. The kinetic data obtained for Ag surface densities lower than 0.7 $Ag/nm^2_{Al_2O_3}$ also suggest that the interaction between NO_x and C_3H_6 adspecies would be rate determining in the C_3H_6-SCR process.

1. Introduction

Since the late 1970s, the preservation of the air quality has become one of the major concerns for the OECD (Organization for Economic Co-operation and Development) countries in order to minimize the impact of air pollutants on environment and health. In Europe in particular, the Euro 6 standards, expected to enter into force in January 2014, will mainly further reduce the NO_x ($NO + NO_2$) emissions from diesel automotives, from 180 to 80 mg/km [1]. To meet these ever more stringent standards, further improvements in the efficiency of the catalytic converters are required.

As emphasized earlier [2], the catalytic reduction of NO_x to N_2 in a strongly oxidizing medium is not trivial. The selective catalytic reduction of NO_x by the hydrocarbons (HC-SCR) would be an elegant alternative to the selective catalytic reduction of NO_x by NH_3 (NH_3-SCR) and the lean NO_x trap (LNT) technologies, which both exhibit intrinsic shortcomings such as the NH_3 slip and CO_2 penalties, respectively. Among the catalytic formulations evaluated to date, Ag/Al_2O_3 has been reported to be the most promising catalyst in the pioneering work by Miyadera [3]. In this study, it was shown that NO_x could be efficiently and selectively reduced to N_2 by various hydrocarbons in the presence of water and in a large excess of O_2. Yet the use of such Ag/Al_2O_3 catalysts is limited because of

* Corresponding author at: Sorbonne Universités, UPMC Univ Paris 06, UMR 7197, Laboratoire de Réactivité de Surface, 4 Place Jussieu, Case 178, F-75005 Paris, France. Tel.: +33 1 44 27 36 30; fax: +33 1 44 27 60 33.
E-mail address: cyril.thomas@upmc.fr (C. Thomas).

http://dx.doi.org/10.1016/j.apcatb.2014.03.025
0926-3373/

the restricted operating temperature window (300–500 °C) within which these materials efficiently catalyze the HC-SCR reaction [2,3], as exhausts temperatures as low as 150 °C are typically encountered in the catalytic converters of diesel cars [4]. Improved HC-SCR efficiencies at the lower temperatures have been obtained with higher hydrocarbons [5,6] or ethanol [7], but, despite the observed broadening of the operating temperature window with the higher hydrocarbons, the Ag/Al_2O_3 catalysts do not meet the SCR efficiencies needed at the lower temperatures yet [8].

The discovery of a low-temperature promoting effect of H_2 on the HC-SCR of NO_x by Satokawa et al. for C_1–C_4 hydrocarbons [9,10], which was later confirmed for higher hydrocarbons [2,11,12], is undoubtedly a major breakthrough for alumina-supported silver catalysts. Interestingly, the H_2 effect has been shown to be specific to Ag/ZSM-5 [13] and Ag/Al_2O_3 [10], as Ag/SiO_2, Ag/TiO_2 and Ag/ZrO_2 were found to be inactive in the presence of H_2 in the C_3H_8-SCR feed [10]. This prompted the importance of aluminum species and the potential contribution of Al_2O_3 in the HC-SCR process as outlined by several groups [14,15].

Recently, the characterization of the Al_2O_3 supporting oxide of a series of Ag/Al_2O_3 samples, via a newly-developed characterization method: namely the temperature-programmed desorption of NO_x [16,17], allowed us to provide further insights into the origin of the optimum loading of Ag on Al_2O_3 for the C_3H_6-SCR of NO_x [18], reported to be about 2 wt% in most studies [3,19–24]. We came to the conclusion that this particular Ag loading resulted from the maximum loading of silver per unit surface area of Al_2O_3 (Ag surface density concept) for which Ag_2O clusters remain highly dispersed on freshly calcined samples [18]. To our knowledge, the influence of the Ag loading on the H_2-promoted HC-SCR of NO_x has been the subject of a very limited number of investigations [24,25], most of the works in this field reporting on Ag/Al_2O_3 samples with a nominal Ag loading close to 2 wt% [2,6]. Sadokhina et al. [24] and Shimizu et al. [25] concluded to an optimum Ag loading of 2 wt% in the H_2-C_6H_{14}-SCR and H_2-C_3H_8-SCR reactions in the presence of 0.1% and 0.5% H_2, respectively. In these works the aliquots of catalysts evaluated in the H_2-HC-SCR reactions were either kept constant [24] or varied to maintain conversions below 30% [25] so that the amounts of Ag changed in the experiments performed. This brings about additional complexity in the interpretation of the catalytic data, especially when those are expressed as NO_x conversions [24] or rates of NO reduction [25] per g of Ag/Al_2O_3 sample. Additionally, Shimizu et al. reported on the NO reduction rates as a function of the Ag loading of the Ag/Al_2O_3 catalysts at a given temperature (300 °C) [25], whereas Sadokhina et al. showed that the catalytic activity of the investigated Ag/Al_2O_3 samples was influenced significantly by the reaction temperature and preferred to provide comparison of the catalysts over a wide range of reaction temperatures (100–550 °C) [24].

The aim of the present work is to gain further understanding on the influence of the Ag loading of Ag/Al_2O_3 samples in the H_2-assisted C_3H_6-SCR of NO_x (H_2-C_3H_6-SCR). For this purpose, and as done in our earlier study on the C_3H_6-SCR of NO_x [18], the amount of Ag in the aliquots of samples evaluated in H_2-C_3H_6-SCR was kept constant via dilution of the Ag/Al_2O_3 catalysts with the bare Al_2O_3 oxide. This study also reports on original findings in the influence of Ag loading on the kinetics of H_2-C_3H_6-SCR that help explaining the observed catalytic trend in the H_2-promoted C_3H_6-SCR reaction.

2. Experimental

2.1. Catalyst synthesis and characterization

The series of Ag/Al_2O_3 samples investigated in the catalysis study corresponds to that used and characterized earlier in the C_3H_6-SCR study [18]. The γ-Al_2O_3 support (Procatalyse, 180 m^2/g) was ground and sieved, and the fraction between 0.200 and 0.315 mm was used to prepare the Ag-promoted samples. The deposition of Ag was performed by incipient wetness impregnation of the bare Al_2O_3 support (0.7 cm^3/g porous volume) with aqueous solutions of $AgNO_3$ (Aldrich, >99%) to achieve silver loadings varying from 0.5 to 4.3 wt%, which were ascertained by inductively coupled plasma atomic emission spectroscopy (ICP-AES, CNRS–Solaize). After impregnation, the Ag-loaded samples were aged for 4 h under ambient conditions and subsequently dried at 100 °C overnight. Finally, the Ag-loaded samples were calcined at 600 °C (3 °C/min) for 4 h in a muffle furnace. From here on, the samples will be denoted as $Ag(x)/Al_2O_3$, where x represents the Ag surface density expressed as the number of Ag atoms per nm^2 of support ($Ag/nm^2_{Al_2O_3}$) [18]. The Ag loadings of Ag(0.0)/, Ag(0.1)/, Ag(0.3)/, Ag(0.4)/, Ag(0.6)/, Ag(0.7)/, Ag(0.8)/, Ag(0.9)/, Ag(1.1)/and Ag(1.3)/Al_2O_3 amounted to 0.0, 0.5, 0.9, 1.3, 1.8, 2.2, 2.6, 3.1, 3.5 and 4.3 wt%, respectively [18].

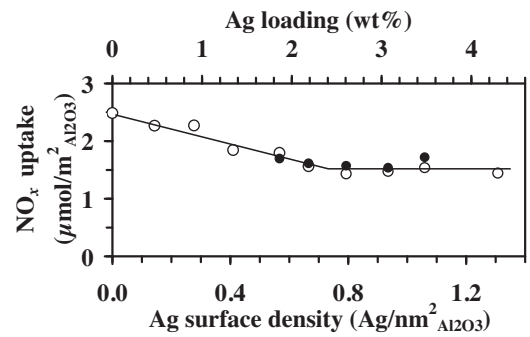

Fig. 1. NO_x uptakes as a function of the Ag surface density/Ag loading: (●) newly synthesized Ag/Al_2O_3 samples and (○) data extracted from [18].

Ag(0.6)/, Ag(0.7)/, Ag(0.8)/Ag(0.9)/and Ag(1.1)/Al_2O_3 samples were newly prepared according to the above-mentioned procedure to be investigated by electron microscopy techniques after being characterized by the NO_x-TPD method described in Refs. [16–18]. The Ag loading and the BET surface area of the newly-prepared samples were measured using an X-ray fluorescence (XRF) spectrometer XEPOS HE (AMETEK) and a Belsorp max (Bell Japan) equipments, respectively. The characterization of these newly-prepared samples by the NO_x-TPD method was in excellent agreement with that reported earlier [18] within the limits of accuracy of the technique (Fig. 1), thus attesting for the reproducibility of the preparation method. These particular silver loadings were selected on the basis of the earlier NO_x-TPD results which suggested that Ag remained in an optimum dispersed state on freshly calcined samples up to an Ag surface density of about 0.7 Ag/nm^2 [18].

Bright field TEM and energy dispersive X-ray spectroscopy (EDS) (PGT detector) characterization of Ag(0.6)/ and Ag(1.1)/Al_2O_3 was performed using a JEOL 2010 microscope operating at 200 kV equipped with an Orius CCD camera (Gatan). Aberration-corrected scanning transmission electron microscopy (STEM) imaging was carried out at the University of Birmingham using a 200 kV JEOL 2100F microscope, fitted with a high angle annular dark field (HAADF) detector and a Bruker EDS detector. For the purposes of imaging the samples were dropped, in dry powder form, onto amorphous carbon-coated copper TEM grids. For comparison purposes, the Ag(0.7)/Al_2O_3 sample was also deposited on a TEM grid after being dispersed in ethanol.

2.2. H_2-C_3H_6-SCR runs

The steady state catalytic H_2-C_3H_6-SCR experiments were carried out in a U-type quartz reactor (12 mm i.d.). It is important

to note that unless specified otherwise and in contrast with most studies published to date, the amount of silver introduced in the catalyst beds remained essentially constant. The samples were held on plugs of quartz wool and consisted in 0.38 g of mechanical mixtures of Ag(x)/Al_2O_3 and Al_2O_3 of the same grain sizes in which the amount of Ag was equal to 30.9 ± 1.2 μmol. The temperature of the tubular furnace was set by a Eurotherm 2408 temperature controller using a K type thermocouple. Prior to the H_2-assisted C_3H_6-SCR experiments, the samples were calcined in situ in O_2 (20%)–He at 550 °C (3 °C/min) for 2 h with a flow rate of 100 mL_{NTP}/min. After cooling down to 150 °C, the samples were submitted to a C_3H_6-SCR experiment from 150 to 550 °C [18]. The samples were subsequently exposed to the H_2-C_3H_6-SCR feed at 150 °C. H_2 (2%/He), NO (4000 ppm/He), C_3H_6 (2000 ppm/He), O_2 (100%) and He (100%) were fed from independent cylinders (Air Liquide) without any further purification via mass flow controllers (Brooks 5850TR). Typically, the composition of the H_2-NO_x-C_3H_6-O_2-He feed was: 0.21% H_2, 385 ppm NO_x (~96% NO), 400 ppm C_3H_6 and 8% O_2 in He, and the total flow rate was 230 mL_{NTP}/min. The temperature was then increased stepwise from 150 to 550 °C with 25 °C increments and left for about 1 h at each temperature step. The reactor outflow was analyzed using a μ-GC (Agilent Technologies, CP4900) equipped with two channels. The first channel, a 5A molecular sieve column (80 °C, 150 kPa He, 200 ms injection time, 30 s backflush time), was used to separate H_2, N_2, O_2 and CO. The second channel, equipped with a poraplot Q column (60 °C, 150 kPa He, 200 ms injection time), was used to separate CO_2, N_2O, C_3H_6 and H_2O. A chemiluminescence NO_x analyzer (Thermo Environmental Instruments 42C-HT) allowed the simultaneous detection of both NO and NO_2. NO_x conversions to N_2 and N_2O were calculated as follows:

$$X_{NO_x \text{ to } N_2}(\%) = (2 \times [N_2])/[NO_x]_{inlet}) \times 100 \quad (1)$$

$$X_{NO_x \text{ to } N_2O}(\%) = (2 \times [N_2O])/[NO_x]_{inlet}) \times 100 \quad (2)$$

where $[NO_x]_{inlet}$, $[N_2]$ and $[N_2O]$ were the concentrations in NO_x measured at the inlet of the reactor and in N_2 and N_2O at the outlet of the reactor. C_3H_6 conversions were calculated on the basis of the CO_x (CO + CO_2) products formed:

$$X_{C_3H_6}(\%) = ([CO] + [CO_2])/([C_3H_6]_{inlet} \times 3) \times 100 \quad (3)$$

where [CO], $[CO_2]$ and $[C_3H_6]_{inlet}$ were the concentrations of CO and CO_2 measured at the outlet of the reactor and that of C_3H_6 measured at the inlet of the reactor, respectively.

The comparison of the catalytic performances of the materials investigated in the present study was also made on the basis of an efficiency criterion (%) in the reduction of NO_x to N_2 in the 150–550 °C range of temperatures. This criterion compares the catalytic performances of the investigated samples to those of a catalyst that would allow for the full reduction of NO_x to N_2 from 150 to 550 °C (100% efficiency).

2.3. Kinetic measurements

Prior to the kinetic measurements, the samples were calcined in situ in O_2 (20%)–He at 550 °C (3 °C/min) for 2 h with a flow rate of 100 mL_{NTP}/min and the temperature was cooled down to 325 °C. In the H_2-C_3H_6-SCR kinetic investigations, the amount of Ag(x)/Al_2O_3 catalysts diluted in Al_2O_3, to obtain catalyst beds of 0.38 g of the corresponding mechanical mixtures, varied from 1 to 5 mg to maintain the conversions of NO_x, C_3H_6 and H_2 below 13%, 16% and 30%, respectively. For comparison purposes, C_3H_6-SCR kinetics was also studied on a mechanical mixture of 0.15 g of Ag(0.7)/Al_2O_3 (2.2 wt% Ag) and 0.23 g of Al_2O_3 at 325 and 375 °C. In this case, the conversions of both NO_x and C_3H_6 varied from 5 to about 30% when the temperature was increased from 325 to 375 °C. At 325 °C, the conversions of NO_x and C_3H_6 on 0.38 g of the bare Al_2O_3 support in the C_3H_6-SCR and H_2-C_3H_6-SCR reactions were found to be about 3% and 2%, respectively. After being pretreated, the samples were contacted with the standard reacting mixture (0.21% H_2, 385 ppm NO_x, 400 ppm C_3H_6 and 8% O_2 in He) used in the H_2-C_3H_6-SCR runs (Section 2.2) for 1–2 h at 325 °C. After reaching steady-state, the determination of the kinetic parameters (α, β, γ and E_a) was performed on the basis of the following power rate law equation:

$$r_{N_2} = k[NO]^{\alpha}[C_3H_6]^{\beta}[H_2]^{\gamma} = A\exp(-E_a/RT)[NO]^{\alpha}[C_3H_6]^{\beta}[H_2]^{\gamma} \quad (4)$$

where r_{N_2}, k, [NO], $[C_3H_6]$, $[H_2]$, α, β, γ, A, E_a, R and T are the rate of reduction of NO_x to N_2 (mol/s g), the kinetic constant, the inlet concentrations in NO, C_3H_6 and H_2, the reaction orders with respect to NO, C_3H_6 and H_2, the pre-exponential factor, the apparent activation energy (J/mol), the gas constant (8.314 J/mol K) and the reaction temperature (K), respectively.

The determination of the reaction orders with respect to NO, C_3H_6 and H_2 was performed at 325 °C by varying the concentration of one of these reactants while the concentrations of the others were kept constant. The following ranges of concentrations were used: 200–700 ppm NO, 200–700 ppm C_3H_6 and 1400–2400 ppm H_2. Note that the influence of O_2 was not investigated and its concentration was maintained to 8%. The reaction orders were determined from the slope of the straight lines obtained by plotting the logarithm of the rate of N_2 production as a function of the logarithm of the concentration of the investigated reactant. The rate of N_2 production (Eq. (5)) was proportional to the conversion of NO_x to N_2 (Eq. (1)) and calculated as follows:

$$r_{N_2} = F_{NO_x} X_{NO_x \text{ to } N_2}/W \quad (5)$$

where F_{NO_x}, $X_{NO_x \text{ to } N_2}$ and W are the NO_x molar flow rate (mol/s), the conversion of NO_x to N_2 (Eq. (1)) and the catalyst loading (g), respectively. It was also verified that the N_2 reaction rates obtained initially under the standard conditions (0.21% H_2, 385 ppm NO_x, 400 ppm C_3H_6 and 8% O_2 in He) were not affected by the changes in the concentrations in the reacting feeds used for the determination of the different reaction orders.

Apparent activation energies were estimated from the slope of the straight lines obtained in the Arrhenius-type plots under the standard feed (0.21% H_2, 385 ppm NO_x, 400 ppm C_3H_6 and 8% O_2 in He) at reaction temperatures in the 325–375 °C range with increments of 10 °C.

The presence of external and internal diffusion limitations was verified according to the criteria defined by Koros–Nowak [26]. External diffusion limitations were checked by changing the amount of Ag(0.7)/Al_2O_3 introduced in the reactor while keeping a constant flow rate to catalyst loading ratio. The H_2-C_3H_6-SCR data obtained under the standard conditions (0.15 g Ag(0.7)/Al_2O_3 + 0.23 g Al_2O_3 and a total flow rate of 230 mL_{NTP}/min) were compared to those obtained for an H_2-C_3H_6-SCR reaction in which the amounts Ag(0.7)/Al_2O_3 and Al_2O_3, and the flow rate were half of those of the standard conditions (0.08 g Ag(0.7)/Al_2O_3 + 0.11 g Al_2O_3 and a total flow rate of 115 mL_{NTP}/min) (Fig. 2a). Internal diffusion limitations were investigated by changing the grain size of a Ag(0.8)/Al_2O_3 catalyst from 50–125 to 200–315 μm (Fig. 2b), while keeping a constant flow rate to catalyst loading ratio (0.12 g Ag(0.8)/Al_2O_3 + 0.26 g Al_2O_3 and a total flow rate of 230 mL_{NTP}/min). The NO_x and C_3H_6 conversions plotted in Fig. 2 indicate the absence of both external and internal diffusion limitations under the present experimental conditions. Comparable experiments carried out for the C_3H_6-SCR reaction also suggested the absence of diffusion limitations in the absence of H_2 in the reacting feed (not shown).

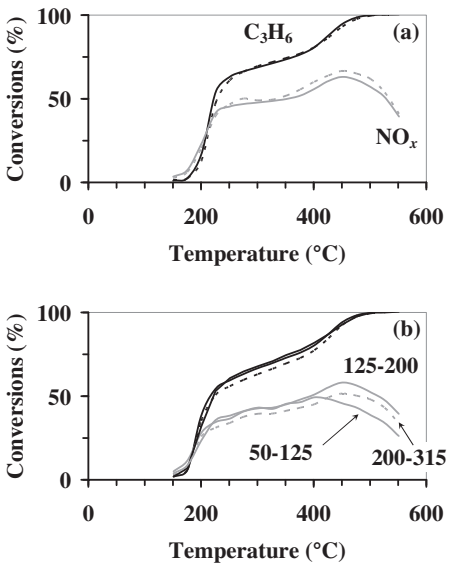

Fig. 2. Examination of the external (a) and internal (b) diffusion limitations in the reduction of NO_x to N_2 (gray curves) and the oxidation of C_3H_6 to CO_x (black curves) in the H_2-C_3H_6-SCR reaction. Feed composition: 0.21% H_2, 385 ppm NO_x, 400 ppm C_3H_6, 8% O_2 and He balance. Mechanical mixtures of (a) 0.15 g Ag(0.7)/Al_2O_3 + 0.23 g Al_2O_3 and 230 mL_{NTP}/min (—), and 0.08 g Ag(0.7)/Al_2O_3 + 0.11 g Al_2O_3 and 115 mL_{NTP}/min (- - -), and (b) 0.12 g Ag(0.8)/Al_2O_3 + 0.26 g Al_2O_3 and 230 mL_{NTP}/min with 50–125 and 125–200 (—), and 200–315 μm (- - -) particle sizes.

3. Results and discussion

3.1. TEM and HAADF-STEM characterization of the post-NO_x-TPD samples

A thorough TEM examination of Ag(0.6)/Al_2O_3 and Ag(1.1)/Al_2O_3, previously characterized by NO_x-TPD, could not reveal unambiguously the presence of Ag and/or Ag_2O clusters on these samples, although the presence of Ag was confirmed in various areas on both samples by means of EDS analyses (not shown). As the poor contrast of Ag and/or Ag_2O clusters on Al_2O_3 may account for the difficulty in their observation, further characterization of the samples exhibiting Ag surface densities ranging from 0.6 to 1.1 Ag/nm^2 was performed by HAADF-STEM. As in the case of the TEM investigation, it was found to be extremely difficult to observe any Ag and/or Ag_2O clusters on all samples with HAADF-STEM. Ag and/or Ag_2O clusters of about 1 nm could thereby be seen on only one area of the Ag(0.6)/Al_2O_3 sample (examples of clusters are highlighted in Fig. 3a). Interestingly when the Ag(0.7)/Al_2O_3 sample was deposited onto the TEM grid from an ethanol suspension, large Ag particles (>10 nm) could be clearly seen on all areas investigated (Fig. 3b and c), whereas no comparable larger particles were observed on the samples deposited in a dry powder form. This observation is consistent with earlier studies of Sayah et al. [27] in which it was concluded that the use of ethanol to disperse Ag/Al_2O_3 samples on TEM grids should be avoided, as doing such leads to the reduction of highly dispersed oxidized Ag species by ethanol and the corresponding formation of large Ag particles which are found to be not representative of the state of Ag in the investigated samples. The larger size of these particles allowed EDS characterization, a typical example of which is shown in Fig. 3c.

To summarize, the characterization of our Ag/Al_2O_3 samples by electronic microscopy techniques shows that Ag is present in a highly dispersed state on Al_2O_3. Such a conclusion is consistent with earlier XAS (X-ray absorption spectroscopy) studies in which it was shown that Ag was almost atomically dispersed after calcination when supported on Al_2O_3 [25,28].

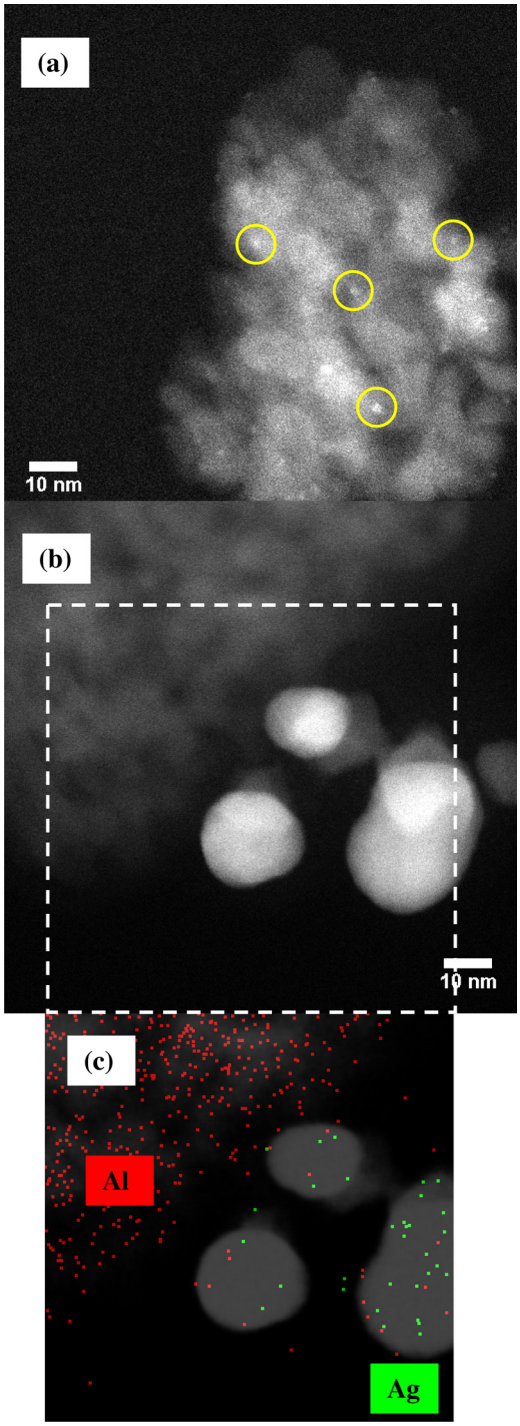

Fig. 3. HAADF-STEM images of post-NO_x-TPD samples: (a) Ag(0.6)/Al_2O_3 deposited on the TEM grid in dry powder form (with some example clusters ringed) and (b) Ag(0.7)/Al_2O_3 deposited on the TEM grid with an ethanol suspension. (c) EDS elemental map overlaid onto (b, dotted square) in which the Al and Ag signals are shown respectively in red and green. (For interpretation of references to color in this figure legend, the reader is referred to the web version of the article).

3.2. Catalytic performances

The influence of the addition of H_2 on the C_3H_6-SCR catalytic performances of the Ag(x)/Al_2O_3 catalysts is illustrated in Fig. 4. In agreement with earlier data of Zhang et al. [29], the addition of

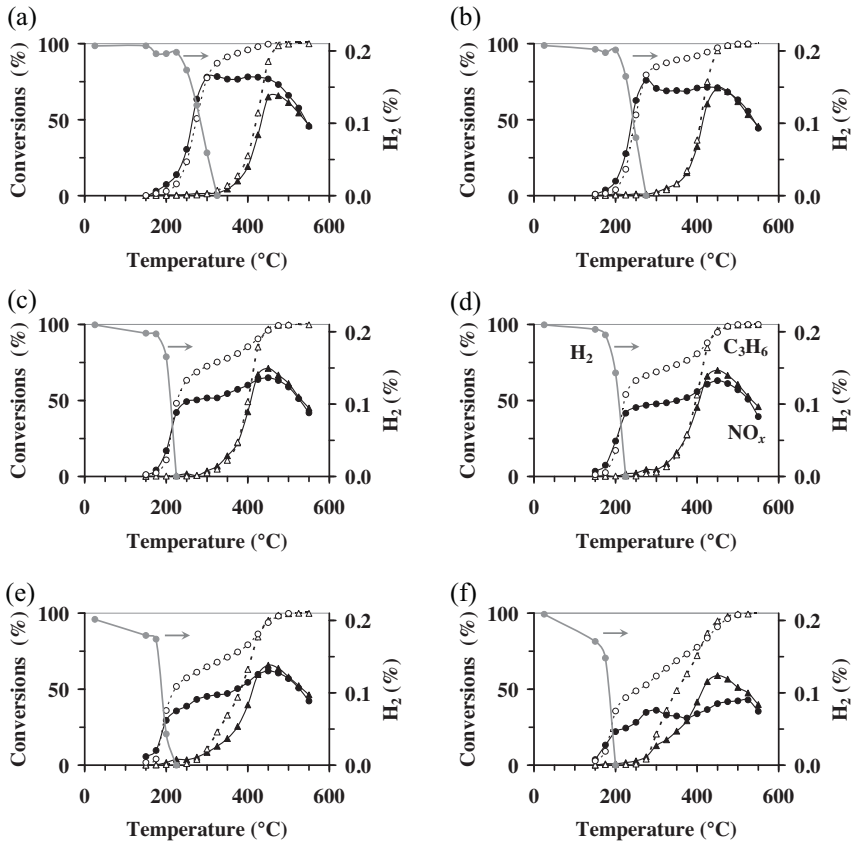

Fig. 4. Influence of the addition of 0.21% H_2 on the conversions of NO_x to N_2 (—) and C_3H_6 to CO_x (- - -) (C_3H_6-SCR (▲, △) and H_2-C_3H_6-SCR (●, ○) reactions) on (a) Ag(0.3)/Al_2O_3, (b) Ag(0.4)/Al_2O_3, (c) Ag(0.6)/Al_2O_3, (d) Ag(0.7)/Al_2O_3, (e) Ag(0.8)/Al_2O_3 and (f) Ag(1.1)/Al_2O_3 for mechanical mixtures of Ag(x)/Al_2O_3 catalysts and Al_2O_3 for which the amount of Ag was kept essentially constant to 30.9 ± 1.2 μmol. Feed compositions: 0% or 0.21% H_2, 385 ppm NO_x, 400 ppm C_3H_6, 8% O_2 and He balance with a 230 mL_{NTP}/min flow rate. The concentration of H_2 in the course of the H_2-C_3H_6-SCR reaction is also shown (-●-).

H_2 drastically promoted the C_3H_6-SCR reaction for temperatures lower than 400 °C. Overall, the addition of 0.21% H_2 in the feed shifted the NO_x to N_2 and C_3H_6 to CO_x conversions to temperatures approximately 150 °C lower than those obtained in the C_3H_6-SCR reaction. On Ag(0.7)/Al_2O_3 (Fig. 4d), the conversions of NO_x and C_3H_6 increased steeply from 150 to 225 °C in the presence of H_2 in the feed, while this sample hardly catalyzed the C_3H_6-SCR reaction from 150 to 300 °C. For temperatures increasing from 225 to 400 °C, the conversions of NO_x and C_3H_6 also increased in the presence of H_2 but to a much more limited extent than from 150 to 225 °C. The pseudo plateau observed in the conversions of NO_x and C_3H_6 in the 225–400 °C region corresponded to a temperature domain for which H_2 was fully consumed (Fig. 4d). For temperatures higher than 400 °C, the conversions of NO_x and C_3H_6 were no longer significantly influenced by the presence of H_2 in the feed. Comparable comments can be made on the other investigated samples (Fig. 4). On Ag(1.1)/Al_2O_3, however, the catalytic performances were found to be higher in C_3H_6-SCR compared to those in H_2-C_3H_6-SCR from 400 to 500 °C (Fig. 4f).

The catalytic performances of the Ag(x)/Al_2O_3 samples in the H_2-C_3H_6-SCR of NO_x are compared in Fig. 5. It can be seen that the NO_x reduction temperature window broadened to lower temperatures as the Ag surface density (Ag loading) increased (Fig. 5a). In parallel, the maximum in N_2O conversion and the conversion of C_3H_6 shifted to lower temperatures as the Ag surface density increased (Fig. 5b and c). The broadening of the NO_x reduction activity to lower temperatures occurred, however, at the expense of the NO_x conversions at the higher temperatures (Fig. 5a). This illustrates how complex is the comparison of the catalytic performances of Ag/Al_2O_3 catalysts with various Ag surface densities (Ag loadings) over a broad temperature domain (150–550 °C).

Fig. 6a shows that plotting the NO_x conversions as a function of the Ag surface density at a given reaction temperature does not allow for an easy comparison of the samples. Indeed, it can be seen in this figure that the Ag surface density providing optimum conversion of NO_x to N_2 in the H_2-C_3H_6-SCR reaction decreases from 0.8 to 0.3 $Ag/nm^2_{Al_2O_3}$ as the temperature increases from 200 to 300 °C. This may be attributed to differences in the conversions of C_3H_6 and H_2, in particular, and to the fact that these conversions varied significantly on the samples investigated (Fig. 4). The comparison of the SCR performances of a series of catalysts at a given reaction temperature should be made ideally with the same level of conversions for all reactants. Note that this is particularly challenging when two reactants of very different reactivity are used, such as H_2 and hydrocarbons in the H_2-HC-SCR reaction. In a H_2-C_3H_8-SCR study performed at 300 °C, Shimizu et al. [25] suggested the existence of an optimum loading of Ag at about 2 wt%. Despite the fact that these authors reported that the corresponding H_2-C_3H_8-SCR reaction rates were measured under conditions where conversions were below 30%, it is uncertain that the term "conversions" also included that of H_2. It must be emphasized that most of the literature data in the H_2-HC-SCR field usually do not report on the conversion of H_2. In agreement with the data shown in Fig. 4, Richter et al., who were among the very few authors to provide the H_2 conversions, also observed an increase in the H_2 consumption in the H_2-C_3H_8-SCR reaction as the Ag loading increased [30].

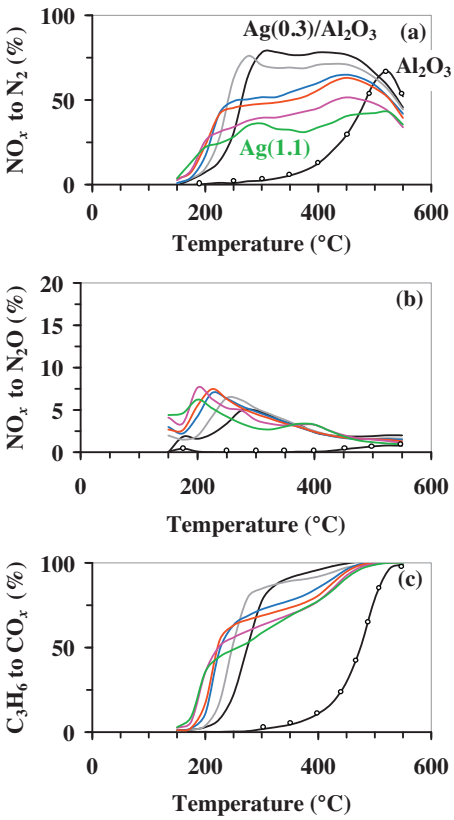

Fig. 5. Influence of Ag surface density of Ag(x)/Al_2O_3 catalysts on the conversions of (a) NO_x to N_2, (b) NO_x to N_2O and (c) C_3H_6 to CO_x in the H_2-C_3H_6-SCR of NO_x on Al_2O_3 (--○--), and Ag(0.3)/Al_2O_3 (black), Ag(0.4)/Al_2O_3 (gray), Ag(0.6)/Al_2O_3 (blue), Ag(0.7)/Al_2O_3 (red), Ag(0.8)/Al_2O_3 (purple) and Ag(1.1)/Al_2O_3 (green) for mechanical mixtures of Ag(x)/Al_2O_3 catalysts and Al_2O_3 for which the amount of Ag was kept essentially constant to 30.9 ± 1.2 μmol. Feed composition: 0.21% H_2, 385 ppm NO_x, 400 ppm C_3H_6, 8% O_2 and He balance with a 230 mL_{NTP}/min flow rate. (For interpretation of references to color in this figure legend, the reader is referred to the web version of the article).

The comparison of the catalytic performances of the materials investigated in the present study was also made on the basis of an efficiency criterion in the reduction of NO_x to N_2 in the 150–550 °C range of temperatures. As illustrated in Fig. 6b, this criterion is defined, for a given catalyst, as the ratio of the area under the NO_x to N_2 conversion curve between 150 and 550 °C to the area under the same curve assuming 100% conversion, for the same range of temperature (i.e. the area of the dotted square in Fig. 6b). This criterion is expressed as a percentage. Fig. 6c firstly shows that the use of such a criterion allows concluding to an optimum Ag surface density of 0.7 Ag/$nm^2_{Al_2O_3}$ (Ag loading of 2.2 wt%) in the C_3H_6-SCR reaction (open symbols). This is in agreement with earlier literature reports in which it was claimed that optimum NO_x reduction activity was obtained for Ag/Al_2O_3 samples with an Ag loading close to 2 wt% [3,18–24]. Fig. 6c also clearly illustrates that the catalytic performances in the C_3H_6-SCR of the Ag(x)/Al_2O_3 samples were drastically promoted by the addition of H_2, as the NO_x reduction to N_2 efficiencies in the H_2-C_3H_6-SCR reaction (full symbols: 55–32%) were found to be much higher than those in the C_3H_6-SCR reaction (open symbols: 20–27%). In contrast to the C_3H_6-SCR reaction, Fig. 6c allows concluding that the concept of optimum Ag surface density (Ag loading) does not apply to the H_2-C_3H_6-SCR reaction over a broad temperature domain (150–550 °C), since increasing NO_x reduction efficiencies were obtained with decreasing Ag surface densities. This conclusion differs substantially from those reported by Sadhokina et al. [24] and Shimizu et al. [25] for whom an optimum Ag loading close to 2 wt% was identified in the H_2-promoted C_6H_{14}- and C_3H_8-SCR reactions, respectively. It cannot be excluded that the nature of the reducing hydrocarbons [2] may be at the origin of the discrepancy within the results of the present work. It must also be recalled that contrary to the procedure followed in the present work (constant silver contents in the aliquots of samples tested), the data reported by Sadhokina et al. [24] and Shimizu et al. [25] were obtained with Ag/Al_2O_3 aliquots in which the amounts of Ag varied, thus bringing additional complexity in the interpretation of the data. To mimic the experimental conditions used by Sadhokina et al. [24] and Shimizu et al. [25], the catalytic performances of aliquots of samples in which the amounts of Ag(x)/Al_2O_3 catalysts (with x = 0.3 and 0.6 Ag/$nm^2_{Al_2O_3}$) diluted with Al_2O_3 were kept constant (0.19 g Ag(x)/Al_2O_3 + 0.19 g Al_2O_3) were investigated

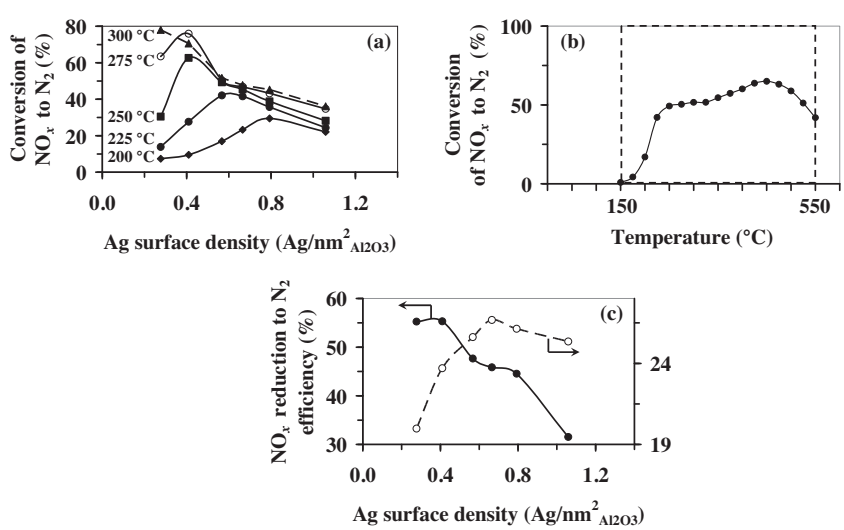

Fig. 6. (a) conversion of NO_x to N_2 in the H_2-C_3H_6-SCR reaction for given reaction temperatures: 200 (–♦–), 225 (–●–), 250 (–■–), 275 (–○–) and 300 °C (- -▲- -), (b) description of the NO_x reduction efficiency criterion in the H_2-C_3H_6-SCR reaction on Ag(0.6)/Al_2O_3 and (c) NO_x reduction to N_2 efficiencies in the C_3H_6-SCR (- -○- -) and H_2-C_3H_6-SCR (–●–) reactions in the 150–550 °C range of temperatures as a function of the Ag surface density for 0.38 g of mechanical mixtures of Ag(x)/Al_2O_3 and Al_2O_3 for which the amount of Ag was kept essentially constant to 30.9 ± 1.2 μmol. Feed compositions: 0% or 0.21% H_2, 385 ppm NO_x, 400 ppm C_3H_6, 8% O_2 and He balance with a 230 mL_{NTP}/min flow rate.

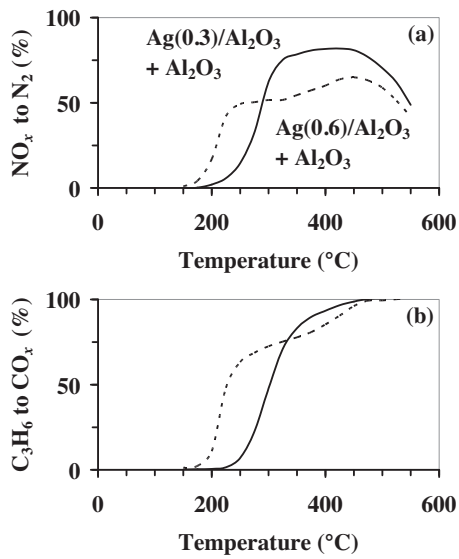

Fig. 7. Influence of the amounts of Ag introduced on the conversions of (a) NO_x to N_2 and (b) C_3H_6 to CO_x in the H_2-C_3H_6-SCR of NO_x on (—) 0.19 g Ag(0.3)/Al_2O_3 + 0.19 g Al_2O_3 (15.4 μmol Ag) and (- - -) 0.19 g Ag(0.6)/Al_2O_3 + 0.19 g Al_2O_3 (31.9 μmol Ag). Feed composition: 0.21% H_2, 385 ppm NO_x, 400 ppm C_3H_6, 8% O_2 and He balance with a 230 mL_{NTP}/min flow rate.

(Fig. 7). As already noticed on aliquots of samples for which the amounts of Ag was kept essentially constant (Fig. 5a and c), Fig. 7 shows a broadening in the NO_x reduction temperature window to lower temperatures at the expense of the NO_x conversions at the higher temperatures and a shift in the conversion of C_3H_6 to lower temperatures as the Ag surface density (Ag loading) increased. As a consequence, the highly-loaded sample (Ag(0.6)/Al_2O_3) is the more active in the NO_x reduction to N_2 at temperatures below 290 °C, whereas it becomes less active than the lowly-loaded sample (Ag(0.3)/Al_2O_3) at higher temperatures (Fig. 7a). Moreover, despite the fact that the amount of Ag in Ag(0.3)/Al_2O_3 (15.4 μmol) was twice lower than that in Ag(0.6)/Al_2O_3 (31.9 μmol), the NO_x reduction to N_2 efficiency estimated for Ag(0.3)/Al_2O_3 (52%) was found to be slightly higher than that of Ag(0.6)/Al_2O_3 (48%). Thus, it appears that the Ag surface density (Ag loading) for which optimum catalytic performances in H_2-C_3H_6-SCR were achieved was strongly dependent on the selected reaction temperature (Figs. 6a and 7a).

3.3. Kinetic investigations

HC-SCR processes have been the subject of a very limited number of kinetic studies [5,20,30–41]. Among these studies, those that have aimed at investigating the kinetics of the H_2-promoted HC-SCR are even scarcer [30,34–36,40] although kinetics has been shown to be extremely profitable in providing unique information about the understanding of the catalytic reactions at a molecular level [26].

Kinetic measurements were performed to gain further insights into the origin of the improved H_2-C_3H_6-SCR catalytic performances obtained with Ag(x)/Al_2O_3 samples of decreasing Ag surface density (Figs. 5a and 6c (–●–)). Fig. 8a shows that the NO reaction order increased from 0.1 to about 0.5 up to a Ag surface density of 0.7 $Ag/nm^2_{Al_2O_3}$ and then levels off at higher Ag surface densities. Fig. 8b indicates that the C_3H_6 reaction order remained essentially constant (0.4) for Ag surface densities lower than or equal to 0.7 $Ag/nm^2_{Al_2O_3}$ and then increased before leveling off (0.8) for Ag surface densities higher than or equal to 0.9 $Ag/nm^2_{Al_2O_3}$. Fig. 8c shows that the H_2 reaction order (0.5) remained essentially constant for Ag surface densities lower than or equal to

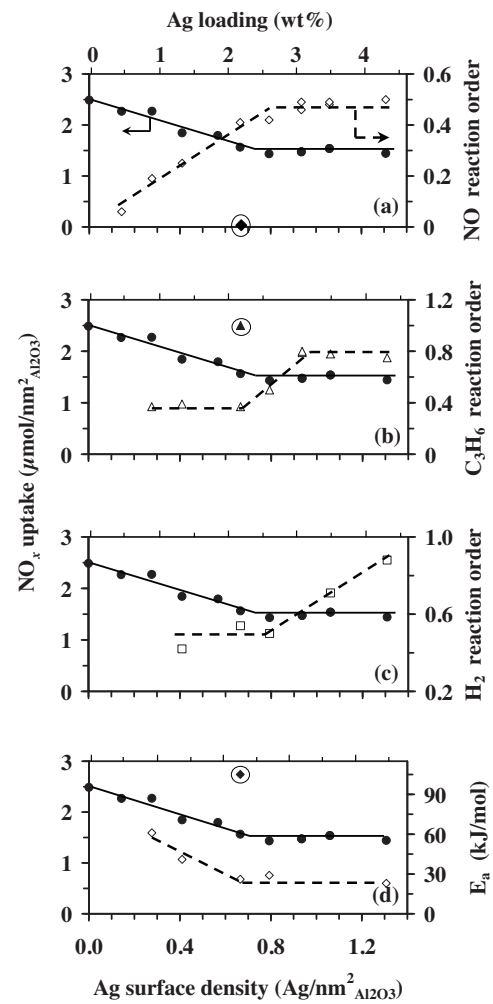

Fig. 8. Influence of Ag surface density of Ag(x)/Al_2O_3 catalysts on the kinetic parameters (a) NO (- -◇- -), (b) C_3H_6 (- -△- -) and (c) H_2 (- -□- -) reaction orders, and (d) apparent activation energies (E_a, - -◇- -) of the H_2-C_6H_6-SCR reaction. The NO_x uptakes determined previously on the freshly calcined samples [18] are also reported (–●–). For comparison purposes, the reaction orders with respect to NO and C_3H_6 and the activation energy measured on Ag(0.7)/Al_2O_3 in the C_3H_6-SCR reaction (absence of H_2) are also reported (circled symbols) in (a), (b) and (c), respectively.

0.8 $Ag/nm^2_{Al_2O_3}$ and then increased up to 0.9 for an Ag surface density of 1.1 $Ag/nm^2_{Al_2O_3}$. Finally, Fig. 8d shows a decrease in the apparent activation energy from 61 to about 26 kJ/mol when the Ag surface density increased from 0.3 to 0.7 $Ag/nm^2_{Al_2O_3}$ before remaining essentially constant up to a Ag surface density of 1.1 $Ag/nm^2_{Al_2O_3}$.

It is remarkable that changes in the reaction orders with respect to NO, C_3H_6 and H_2, and in the apparent activation energy (E_a) for the reduction of NO_x to N_2 in the H_2-C_3H_6-SCR reaction occurred at an Ag surface density (Fig. 8: ~0.7 $Ag/nm^2_{Al_2O_3}$ = 2.2 wt% Ag) coinciding with the changes observed in the NO_x uptakes of the Al_2O_3 support of the Ag(x)/Al_2O_3 catalysts [18].

The kinetic parameters reported in earlier HC-SCR investigations performed on Ag/Al_2O_3 catalysts are summarized in Table 1 in the order of increasing carbon number in the HC reductant. For comparison purposes, the Ag loadings have also been expressed as Ag surface densities according to Ref. [18]. It can be seen from this table that these studies have mainly focused on the determination of the apparent activation energies (E_a) of the HC-SCR process and that the studies in which the NO and HC reactions orders have been determined are rather limited, in particular in the case of the

Table 1
Comparison of the kinetic data reported earlier in the HC-SCR and H_2-HC-SCR of NO_x on Al_2O_3 and Ag/Al_2O_3 catalysts with those obtained in the present study.

			HC-SCR of NO_x			H_2-HC-SCR of NO_x			
Ag[a] (wt%)	δ[b] ($Ag/nm^2_{Al_2O_3}$)	HC	E_a[c] (kJ/mol)	NO[d]	HC[d]	E_a[c] (kJ/mol)	NO[d]	HC[d]	Ref.
0.0	0.0	CH_4	124	–	–	–	–	–	[31]
0.8–21.5	0.2–4.8	CH_4	95–124	–		–	–	–	[31]
2.0	0.7	C_2H_5OH	57 ± 3	−0.28	0.34	–	–	–	[32]
0.0	0.0	C_2H_5OH	47	–	–	–	–	–	[33]
2.1	0.5	C_2H_5OH	39	–	–	–	–	–	[33]
3.5	0.8	C_2H_5OH	37	–	–	–	–	–	[33]
8.0	1.9	C_2H_5OH	39	–	–	–	–	–	[33]
2.0	0.5	C_2H_5OH	166	–	–	116	–	–	[34]
3.8	1.1	$-C_{12}H_{26}-$	123	–	–	89	–	–	[34]
6.2	1.9	$m-$xylene	83	–	–	65	–	–	[34]
0.0	0.0	C_3H_6	85	0.3	0.3				[35]
1.0	0.2	C_3H_8	147	–	–	33	–	–	[30]
5.0	1.1	C_3H_8	250	–	–	30	–	–	[30]
2.0	0.4	C_3H_8	224	−2.53	1.91	61	0.49	0.76	[36]
2.0	0.6	C_6H_{14}	67	0.8	0.9	–	–	–	[20]
2.0	0.6	C_8H_{18}	–	≥0	≥0	–	–	–	[5]
2.0	0.6	C_8H_{18}	–	0	>1.0	–	–	–	[37]
2.0	0.6	C_8H_{18}	–	0	1.0	–	–	–	[38]
1.5	1.2	C_8H_{18}	–	0.5–0.7	0–1.7	–	–	–	[39]
1.9	0.6	C_8H_{18}	–	−0.39	–	–	0.14–0.40	0.26–0.40	[40]
1.9	0.6	$C_{16}H_{34}$	–	0.5–0.6	≥0	–	–	–	[41]
2.2	0.7	C_3H_6	105	0.0	1.0	26	0.4	0.4	This
0.5–4.3	0.1–1.4	C_3H_6	–	–	–	61–23	0.1–0.5	0.4–0.8	study

[a] Ag loading in the Ag/Al_2O_3 catalysts.
[b] Ag surface density corrected for the content of Ag as Ag_2O following the procedure described in Ref. [18].
[c] Apparent activation energies.
[d] Reaction orders with respect to NO and HC for the production of N_2.

H_2-promoted HC-SCR. The kinetic data reported for the first time in Fig. 8 for the H_2-C_3H_6-SCR reactions over an extended range of Ag surface densities are, therefore, of the utmost interest. It can also be deduced from Table 1 that the nature of the hydrocarbons has a significant influence on the kinetic parameters of the HC-SCR reaction. Nevertheless, some common trends can be drawn from these sets of data.

In particular, Richter et al. [30], Kim et al. [34] and Shimizu et al. [36] reported on a significant decrease in E_a with the promotion of the HC-SCR reaction by H_2 (Table 1). This finding can also be observed in Fig. 8d where the E_a of the C_3H_6-SCR reaction decreases tremendously from 105 (circled full diamond) to 26 kJ/mol (open diamond) when promoted by H_2 on $Ag(0.7)/Al_2O_3$. Regarding the evolution of E_a with the Ag loading (Ag surface density), conflicting results were reported by Kim et al. in C_2H_5OH-$C_{12}H_{26}$-*m*-xylene-SCR [34] and Richter et al. in C_3H_8-SCR [30]. Kim et al. [34] concluded to a decrease in E_a, whereas Richter et al. [30] reported on either an increase in E_a in C_3H_8-SCR or constant E_a in H_2-C_3H_8-SCR with increasing loadings of Ag (Table 1). The data plotted in Fig. 8d indicate a decrease in E_a of the H_2-C_3H_6-SCR reaction with increasing Ag loadings, but in a more restricted range of Ag surface densities (0.3–0.7 $Ag/nm^2_{Al_2O_3}$) than that reported by Kim et al. (0.5–1.9 $Ag/nm^2_{Al_2O_3}$) [34].

Regarding the reaction orders, earlier studies concluded that the promotion of the HC-SCR reaction by H_2 led to a significant increase in the NO reaction order [36,40] and a decrease in the reaction order in C_3H_8 [36] for a given Ag loading (0.4–0.6 $Ag/nm^2_{Al_2O_3}$) (Table 1). The data shown in Fig. 8a and b for $Ag(0.7)/Al_2O_3$ are consistent with these findings. The NO reaction order (Fig. 8a) increased from 0 (C_3H_6-SCR, circled full diamond) to 0.4 (H_2-C_3H_6-SCR, open diamond), whereas the C_3H_6 reaction order (Fig. 8b) decreased from 1.0 (C_3H_6-SCR, circled full triangle) to 0.4 (H_2-C_3H_6-SCR, open triangle). To our knowledge, the trends in the NO, C_3H_6 and H_2 reaction orders shown in Fig. 8a–c for an H_2-HC-SCR reaction have not been reported to date.

Before providing interpretation for the evolutions of the kinetic parameters with increasing Ag surface densities (Fig. 8), the main conclusions of the characterization of the $Ag(x)/Al_2O_3$ catalysts by the NO_x-TPD method, and the associated evolution of the NO_x uptakes of the supporting Al_2O_3 oxide (NO_x species do not chemisorb on Ag species) [18], shall be recalled. The decrease in the NO_x uptakes observed with increasing Ag surface densities up to an Ag density of about 0.7 $Ag/nm^2_{Al_2O_3}$ ([18] and Fig. 8), for which optimum C_3H_6-SCR activity was obtained (Fig. 6c, - -○- -), was interpreted as the maximum loading of silver per unit surface area of Al_2O_3 for which optimal Ag dispersion was preserved [18]. The observed linear decrease in the NO_x uptake below an Ag surface density of about 0.7 $Ag/nm^2_{Al_2O_3}$ was also attributed to the formation of homogeneously distributed Ag species of increasing density [18]. For Ag surface densities higher than 0.7 $Ag/nm^2_{Al_2O_3}$, the NO_x uptakes of the Al_2O_3 supporting oxide remained essentially constant (Fig. 8). This was assigned to an increase in the size of the Ag clusters, the Al_2O_3 surface sites onto which Ag was anchored being saturated for an Ag surface density of about 0.7 $Ag/nm^2_{Al_2O_3}$ [18]. Despite the NO_x-TPD characterization of the $Ag(x)/Al_2O_3$ catalysts was done on calcined samples [18], the correlations obtained in the present work between the NO_x uptakes and the changes in the kinetic parameters of the H_2-HC-SCR reaction (Fig. 8) suggest that the Ag species in the calcined samples may be taken as representative of those existing under the reaction conditions from an Ag dispersion point of view. This assumption is supported by the EXAFS studies performed by Shimizu et al. [25] and Burch et al. [28] on Ag/Al_2O_3 samples with Ag loadings of about 2 wt% (Ag surface density of 0.4 $Ag/nm^2_{Al_2O_3}$ in [25]) which concluded to a very limited sintering of the Ag phase under HC-SCR reaction conditions, promoted or not by H_2, and to the preservation of Ag in a highly dispersed state with the formation of Ag clusters made of 3–4 Ag atoms for this particular Ag loading. These earlier studies, together with the characterization of the newly-prepared samples by NO_x-TPD (Fig. 1) and by electronic microscopy techniques (Section 3.1),

for which Ag was shown to remain in a highly dispersed state whatever the silver loading in the dry powder samples, provide support for the use of the Ag surface density concept in the present study.

Fig. 5c clearly demonstrates that the activation of C_3H_6 in the H_2-C_3H_6-SCR reaction occurred on Ag sites, as the bare Al_2O_3 support does not catalyze C_3H_6 oxidation at temperatures as low as those observed for the Ag(x)/Al_2O_3 samples. The much lower conversion of H_2 on Al_2O_3 (<5% at 500 °C, not shown) than those measured on the Ag(x)/Al_2O_3 catalysts (100% above 325 °C, Fig. 4) also indicates that the activation of H_2 occurred on Ag species. These conclusions are consistent with the recently published elegant study of Kim et al. in which the promotional effect of H_2 in HC-SCR was attributed to morphological and chemical changes of the Ag phases [34]. For Ag surface densities lower than or equal to 0.7 Ag/nm$^2_{Al_2O_3}$, the reaction orders of 0.4 in C_3H_6 (Fig. 8b) and 0.5 in H_2 (Fig. 8c) remained essentially constant and positive. Within the same range of Ag surface densities ($<$ 0.7 Ag/nm$^2_{Al_2O_3}$), the NO reaction order increased from 0.1 to 0.4 (Fig. 8a). This indicates that the activated form of NO (NO_x adsorbed species: NO_x adspecies) does not compete for the Ag sites responsible for the activation of C_3H_6 and H_2, as such a competition should have resulted in changes in the reaction orders in C_3H_6 and H_2, which was not observed (Fig. 8b and c). As a consequence, the sites responsible for the adsorption of NO_x are rather related to the Al_2O_3 supporting oxide. This proposal is consistent with earlier FTIR studies in which it was shown that significant amounts of NO_x were stored on the Al_2O_3 supporting oxide [12,34,36,42,43] and it was suggested that nitrates would be reaction intermediates of HC-SCR [20].

The increase in the NO reaction order with the addition of H_2 on Ag(0.7)/Al_2O_3 (Fig. 8a), from 0 for the C_3H_6-SCR to 0.4 for the H_2-C_3H_6-SCR (Fig. 8a), could be assigned to a depletion in the coverage of the NO_x adspecies [2,36] due to the drastic increase in the H_2-C_3H_6-SCR reaction rate compared to that of C_3H_6-SCR at 325 °C (Fig. 4d). The much lower C_3H_6-SCR reaction rate would thus allow for saturation coverage of the Al_2O_3 sites by the NO_x adspecies which would result in the observed 0th reaction order with respect to NO. This explanation would be consistent with the decrease in nitrate coverage with the introduction of H_2 observed by Shimizu et al. [36]. Likewise, the increase in the NO reaction order as the Ag surface density increases (Fig. 8a) is attributed to a decrease in the coverage of the catalyst surface by the NO_x adspecies which is coherent with the observed decrease in the NO_x uptakes of the Ag(x)/Al_2O_3 samples for Ag surface densities lower than 0.7 Ag/nm$^2_{Al_2O_3}$. The observed leveling off of the NO reaction order for Ag surface densities higher than 0.7 Ag/nm$^2_{Al_2O_3}$ can be associated to the constant coverage of the catalyst surface by the NO_x adspecies, in agreement with the steadiness of the NO_x uptakes observed in this Ag surface density domain (Fig. 8a). It would have been of the utmost interest to have been able to provide additional quantitative data supporting the suggested differences in NO_x coverage accounting for the changes observed in the NO reaction order. One may have thought about the use of the SSITKA (Steady-State Isotopic Transient Kinetic Analysis) techniques to provide such information [44]. Recently, Burch and co-workers [45,46] put particular emphasis on the fact that conventional SSITKA should be used with an extreme caution in identifying true reaction intermediates in the H_2-C_8H_{18}-SCR reaction. These difficulties could be overcome for isocyanate intermediates by using short time on stream SSITKA (STOS-SSITKA) instead of conventional SSITKA [45,46]. While the involvement of nitrate-type species adsorbed on or close to the active Ag sites could be revealed by STOS-SSITKA in the H_2-NH_3-SCR reaction [47], no such information could be obtained in the more complex H_2-C_8H_{18}-SCR reaction [46]. These arguments therefore clearly prevent the use of STOS-SSITKA in the

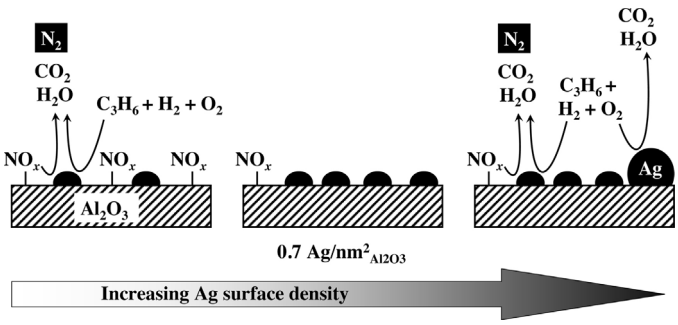

Fig. 9. Schematic representation of the H_2-C_3H_6-SCR reaction on Ag(x)/Al_2O_3 catalysts with increasing Ag surface densities (x).

estimation of the NO_x ad-species involved in the H_2-C_3H_6-SCR process of the present study. Finally, exhausts generally contain high concentrations of CO_2 and H_2O (5–12%). As the NO_x species were deduced to be chemisorbed on Al_2O_3 in the present work, it cannot be excluded that the presence of CO_2 and H_2O in the feed would lead to a decrease in the performances of the Ag/Al_2O_3 catalysts in the SCR reactions due to their competitive adsorption with the NO_x species. In agreement with this, the inhibiting effect of H_2O has been highlighted previously on the C_3H_6-SCR [48–50] and H_2-C_3H_8-SCR [30] performances.

The increase in the C_3H_6 and H_2 reaction orders for Ag surface densities higher than 0.7 Ag/nm$^2_{Al_2O_3}$ (Fig. 8b and c) can be assigned to the fact that the combustion of these molecules on the larger Ag nanoparticles, present at such high Ag loadings and which oxidation capabilities have been clearly illustrated [51], prevails over their efficient use in the SCR reaction for the production of N_2 [3].

The decrease in the apparent activation energy (E_a) with increasing Ag surface densities up to 0.7 Ag/nm$^2_{Al_2O_3}$, also reported recently by Kim et al. [34], is more difficult to explain as the higher E_a (Fig. 8d) were found on the more active samples in H_2-C_3H_6-SCR (Fig. 5a). As recalled by Richter et al. [30] and Bond et al. [52], the rate constant k (Eq. (4)) not only varies with E_a but also with the pre-exponential factor (A), which itself depends on the concentration of active sites. This peculiarity is defined as the so-called compensation phenomenon in catalysis [52]. The unexpected higher activity in the H_2-C_3H_6-SCR reaction of the Ag(x)/Al_2O_3 samples with the lower Ag surface densities, associated to their higher E_a, might be related to the higher number of active sites on the Al_2O_3 supporting oxide able to chemisorb NO_x species in agreement with the NO_x uptake data (Fig. 8), hence to their higher pre-exponential factors. Yet the observed changes in the NO, C_3H_6 and H_2 reaction orders (Fig. 8a–c) prevented the estimation of the corresponding pre-exponential factors. For Ag surface densities higher than or equal to 0.7 Ag/nm$^2_{Al_2O_3}$, E_a remained essentially constant as were the NO_x uptakes (Fig. 8d), and therefore also the number of active sites on the Al_2O_3 supporting oxide able to chemisorb NO_x species and the corresponding pre-exponential factors. The lower catalytic performances of these samples (Fig. 4b) is thus rather assigned to the combustion of C_3H_6 on larger Ag nanoparticles [3] formed at these particularly high Ag surface densities [18].

In summary, the interpretation of the activity and kinetic data led us to conclude that the H_2-C_3H_6-SCR reaction proceeds via the activation of H_2 and C_3H_6 on Ag species which further react with NO_x adspecies activated on the Al_2O_3 support, as schematically illustrated in Fig. 9. Such a proposal is consistent with the conclusions drawn earlier by She and Flytzani–Stephanopoulos on CH_4-SCR studies [31]. The unexpected decrease in the H_2-C_3H_6-SCR performances observed with increasing Ag surface densities (Figs. 5a and 6c) is assigned first to the decrease in the number of

active sites on the Al_2O_3 supporting oxide able to chemisorb NO_x species [18] for Ag surface densities lower than 0.7 $Ag/nm^2_{Al_2O_3}$ and then to the combustion of C_3H_6 on the larger Ag nanoparticles for Ag surface densities higher than 0.7 $Ag/nm^2_{Al_2O_3}$ (Fig. 9). Finally, the kinetic data obtained for Ag surface densities lower than 0.7 $Ag/nm^2_{Al_2O_3}$, in particular, suggest that the interaction between the NO_x and C_3H_6 would be rate determining in the C_3H_6-SCR process in agreement with the earlier proposal of Burch et al. [49].

4. Conclusion

The promotional effect of H_2 in the C_3H_6-SCR reaction was confirmed on a series of $Ag(x)/Al_2O_3$ samples exhibiting various Ag surface densities ($0.3 < x < 1.1$ $Ag/nm^2_{Al_2O_3}$). TEM and HAADF-STEM analyses of the $Ag(x)/Al_2O_3$ catalysts indicated that silver was in a highly dispersed state, whatever the metal loading. The introduction of H_2 resulted in (i) a broadening in the NO_x reduction temperature window to lower temperatures at the expense of the NO_x conversions at temperatures higher than 300 °C and (ii) a shift in the conversion of C_3H_6 to lower temperatures as the Ag surface density increased. In contrast to the C_3H_6-SCR reaction, the concept of optimum Ag surface density at 0.7 $Ag/nm^2_{Al_2O_3}$ (Ag loading of 2.2 wt%) [18] did not apply to the H_2-promoted C_3H_6-SCR reaction over a broad temperature domain. Indeed, the catalytic performances in the H_2-C_3H_6-SCR reaction in the 150–550 °C range of temperatures improved as the Ag surface density of the $Ag(x)/Al_2O_3$ samples decreased. A detailed kinetic study was performed in which the reaction orders in NO, C_3H_6 and H_2, and the apparent activation energies were determined on the $Ag(x)/Al_2O_3$ series. Remarkably, changes in these kinetic parameters were found to occur at an Ag surface density close to 0.7 $Ag/nm^2_{Al_2O_3}$ (Ag loading of 2.2 wt%) coinciding with the changes observed earlier in the NO_x uptakes of the Al_2O_3 supporting oxide [18]. Interpretation of the activity and kinetic data led us to conclude that the H_2-C_3H_6-SCR reaction proceeds via the activation of H_2 and C_3H_6 on Ag species which further react with NO_x adspecies activated on the Al_2O_3 support. The unexpected decrease in the H_2-C_3H_6-SCR performances observed with increasing Ag surface densities was assigned to a decrease in number of active sites on the Al_2O_3 supporting oxide able to chemisorb NO_x species [18] for Ag surface densities lower than 0.7 $Ag/nm^2_{Al_2O_3}$ and to the combustion of C_3H_6 on the larger Ag nanoparticles for Ag surface densities higher than 0.7 $Ag/nm^2_{Al_2O_3}$ (Fig. 9). Finally, the kinetic data obtained for Ag surface densities lower than 0.7 $Ag/nm^2_{Al_2O_3}$ also suggest that the interaction between the NO_x and C_3H_6 would be rate determining in the C_3H_6-SCR process.

Acknowledgments

TC gratefully acknowledges UPMC for financial support (PhD Grant No.: 322/2012). The authors would like to thank the IMPC (Institut des Matériaux de Paris Centre) through the “plateforme de microscopie électronique”. The authors also acknowledge financial support from COST Action MP0903 Nanoalloys. The aberration corrected STEM instrument used in this work was funded by the Birmingham Science City project. RLC and ZYL acknowledge the Engineering and Physical Sciences Research Council U.K. for financial support (Grant No.: EP/G070326/1). J. Olek (Engineer, Agilent Technologies) is acknowledged for his prompt and useful assistance in the use of the μ-GC system.

References

[1] http://ec.europa.eu/environment/air/transport/road.htm
[2] R. Burch, Catal. Rev. Sci. Eng. 46 (2004) 271.
[3] T. Miyadera, Appl. Catal. B: Environ. 2 (1993) 199.
[4] F. Klingstedt, K. Eränen, L.-E. Lindfors, S. Andersson, L. Cider, C. Landberg, E. Jobson, L. Eriksson, T. Ilkenhans, D. Webster, Top. Catal. 30/31 (2004) 27.
[5] K.-I. Shimizu, A. Satsuma, T. Hattori, Appl. Catal. B: Environ. 25 (2000) 239.
[6] K.-I. Shimizu, J. Shibata, A. Satsuma, T. Hattori, Phys. Chem. Chem. Phys. 3 (2001) 880.
[7] S. Kameoka, T. Chafik, Y. Ukisu, T. Miyadera, Catal. Lett. 51 (1998) 11.
[8] C. Petitto, H.P. Mutin, G. Delahay, Appl. Catal. B: Environ. 134–135 (2013) 258.
[9] S. Satokawa, Chem. Lett. 29 (2000) 294.
[10] S. Satokawa, J. Shibata, K.-I. Shimizu, A. Satsuma, T. Hattori, Appl. Catal. B: Environ. 42 (2003) 179.
[11] K.-I. Shimizu, A. Satsuma, Phys. Chem. Chem. Phys. 8 (2006) 2677.
[12] R. Burch, J.P. Breen, C.J. Hill, B. Krutzch, B. Konrad, E. Jobson, L. Cider, K. Eränen, F. Klingstedt, L.-E. Lindfors, Top. Catal. 30/31 (2004) 19.
[13] J. Shibata, Y. Takada, A. Shishi, S. Satokawa, A. Satsuma, T. Hattori, J. Catal. 222 (2004) 368.
[14] K.A. Bethke, H.H. Kung, J. Catal. 172 (1997) 93.
[15] J.H. Lee, S.J. Schmieg, S.H. Oh, Appl. Catal. A: Gen. 342 (2008) 78.
[16] H.Y. Law, J. Blanchard, X. Carrier, C. Thomas, J. Phys. Chem. C 114 (2010) 9731.
[17] C. Thomas, J. Phys. Chem. C 115 (2011) 2253.
[18] T. Chaieb, L. Delannoy, C. Louis, C. Thomas, Appl. Catal. B: Environ. 142–143 (2013) 780.
[19] T.E. Hoost, R.J. Kulda, K.M. Collins, M.S. Chattha, Appl. Catal. B: Environ. 13 (1997) 59.
[20] K.-I. Shimizu, J. Shibata, H. Yoshida, A. Satsuma, T. Hattori, Appl. Catal. B: Environ. 30 (2001) 151.
[21] L.-E. Lindfors, K. Eränen, F. Klingstedt, D. Yu Murzin, Top. Catal. 28 (2004) 185.
[22] K. Arve, L. Čapek, F. Klingstedt, K. Eränen, L.-E. Lindfors, D.Y. Murzin, J. Dědeček, Z. Sobalik, B. Wichterlová, Top. Catal. 30/31 (2004) 91.
[23] R. Zhang, S. Kaliaguine, Appl. Catal. B: Environ. 78 (2008) 275.
[24] N.A. Sadokhina, A.F. Prokhorova, R.I. Kvon, I.S. Mashkovskii, G.O. Bragina, G.N. Baeva, V.I. Bukhtyarov, A. Yu Stakheev, Kinet. Catal. 53 (2012) 107.
[25] K.-I. Shimizu, M. Tsuzuki, K. Kato, S. Yokota, K. Okumara, A. Satsuma, J. Phys. Chem. C 111 (2007) 950.
[26] M. Boudart, G. Djéga-Mariadassou, Kinetics of Heterogeneous Catalytic Reactions, Princeton University Press, Princeton, NJ, 1984.
[27] E. Sayah, D. Brouri, Y. Wu, A. Musi, P. Da Costa, P. Massiani, Appl. Catal. A: Gen. 406 (2011) 94–101.
[28] J.P. Breen, R. Burch, C. Hardacre, C.J. Hill, J. Phys. Chem. B 109 (2005) 4805.
[29] X. Zhang, Y. Yu, H. He, Appl. Catal. B: Environ. 76 (2007) 241.
[30] M. Richter, U. Bentrup, R. Eckelt, M. Schneider, M.-M. Polh, R. Fricke, Appl. Catal. B: Environ. 51 (2004) 261.
[31] X. She, M. Flytzani-Stephanopoulos, J. Catal. 237 (2006) 79.
[32] W.L. Johnson, G.B. Fisher, T.J. Toops, Catal. Today 184 (2012) 166.
[33] Y. Yan, Y. Yu, H. He, J. Zhao, J. Catal. 293 (2012) 13.
[34] P.S. Kim, M.K. Kim, B.K. Cho, I.-S. Nam, S.H. Oh, J. Catal. 301 (2013) 65.
[35] M. Haneda, Y. Kintaichi, H. Shimada, H. Hamada, J. Catal. 192 (2000) 137.
[36] K.-I. Shimizu, J. Shibata, A. Satsuma, J. Catal. 239 (2006) 402.
[37] K. Arve, F. Klingstedt, K. Eränen, J. Wärna, L.-E. Lindfors, D.Yu. Murzin, Chem. Eng. J. 107 (2005) 215.
[38] K. Eränen, L.-E. Lindfors, F. Klingstedt, D.Yu. Murzin, J. Catal. 219 (2003) 25.
[39] J.R. Hernàndez Carucci, A. Kurman, H. Karhu, K. Arve, K. Eränen, J. Wärnå, T. Salmi, D.Yu. Murzin, Chem. Eng. J. 154 (2009) 34.
[40] K. Arve, H. Backman, F. Klingstedt, K. Eränen, D.Yu. Murzin, Appl. Catal. A: Gen. 303 (2006) 96.
[41] K. Arve, J.R. Hernàndez Carucci, K. Eränen, A. Aho, D.Yu. Murzin, Appl. Catal. B: Environ. 90 (2009) 603.
[42] P. Sazama, L. Čapek, H. Drobná, Z. Sobalík, J. Dědeček, K. Arve, B. Wichterlová, J. Catal. 232 (2005) 302.
[43] S. Chansai, R. Burch, C. Hardacre, J.P. Breen, F. Meunier, J. Catal. 276 (2010) 49.
[44] S.L. Shannon, J.G. Goodwin, Chem. Rev. 95 (1995) 677.
[45] S. Chansai, R. Burch, C. Hardacre, J. Breen, F. Meunier, J. Catal. 276 (2010) 49.
[46] S. Chansai, R. Burch, C. Hardacre, J. Breen, F. Meunier, J. Catal. 281 (2011) 98.
[47] S. Chansai, R. Burch, C. Hardacre, J. Catal. 295 (2012) 223.
[48] F.C. Meunier, R. Ukropec, C. Stapelton, J.R.H. Ross, Appl. Catal. B: Environ. 30 (2001) 163.
[49] R. Burch, J.P. Breen, F.C. Meunier, Appl. Catal. B: Environ. 39 (2002) 283.
[50] S.T. Korhonen, A.M. Beale, M.A. Newton, B.M. Weckhuysen, J. Phys. Chem. C 115 (2011) 885.
[51] N. Bogdanchikova, F.C. Meunier, M. Avalos-Borja, J.P. Breen, A. Pestryakov, Appl. Catal. B: Environ. 36 (2002) 287.
[52] G.C. Bond, M.A. Keane, H. Kral, J.A. Lercher, Catal. Rev. Sci. Eng. 42 (2000) 323.